

Statistics of microscopic yielding in sheared aqueous foams

Yuhong Wang, Kapilanjana Krishan, and Michael Dennin

Department of Physics and Astronomy, University of California at Irvine, Irvine, California 92697-4575

(Dated: February 8, 2020)

We detail the statistical distribution of bubble rearrangements in a sheared two-dimensional foam. Such rearrangements, known as T1 events, are vital to mechanisms resulting in flow through microscopic mechanical yielding. We find that at a constant rate of shear, the rate of occurrence of T1 events shows only small fluctuations. This rate is however seen to vary significantly with a variation in the initial configuration of bubbles constituting the foam. In addition, we detail the spatial and orientational distribution of T1 events and relate them to the distribution of stresses in the bulk of the material. Some insights into the irreversibility of the dynamics are also discussed.

PACS numbers:

I. INTRODUCTION

In many materials, the microscopic structure predominantly determines the mechanism of flow. The microscopic response to deformation may vary from linear in the case of elastic materials and newtonian fluids to highly nonlinear in non-newtonian fluids and granular materials. In many materials, the response is linear for sufficiently small deformations, only to become nonlinear at a critical value of the deformation. The transition to nonlinear behavior is often controlled by the nature of various microscopic events. It is worth highlighting just a few examples. In crystalline solids, defects in the lattice structure may lead to fractures within the material [1]. In amorphous materials, plasticity has been described in terms of local rearrangements of particles, known as shear transformation zones (STZs) [2, 3]. For soft materials, such as colloids, foams, and emulsions, a soft glassy rheology (SGR) model based on particle rearrangements is able to capture many features of the macroscopic behavior [4, 5]. Similarly, in the context of emulsions, a model based on “weak” zones within the material has been successful in explaining anomalous measurements of rheological properties [6, 7]. Therefore, characterizing microscopic rearrangements is imperative to understanding the behavior of materials subjected to external loads during stress, strain etc.

In this article we study the behaviour of aqueous foams when subjected to macroscopic shear. The yielding of such foams is typically described by a Bingham model that proposes a critical yield stress at which the material switches from an elastic to a plastic response [8]. When stresses in the material exceed the yield stress, failure in the microscopic structure results in flow within the material. The microscopic aspect related to this behaviour is a succession of slip between the constituent bubbles of the foam, known as T1 events (see Fig. 1). In its most basic manifestation, such slip involves four neighboring bubbles, with one pair of nearest neighbours becoming next-nearest neighbours and vice-versa for another pair. T1 events have been the subject of study in simulations [9, 10, 11, 12], indirect measurement in three-dimensional foam using diffusive wave spectroscopy

(DWS) [13, 14, 15, 16, 17], and direct observation in two-dimensional foams [18, 19, 20].

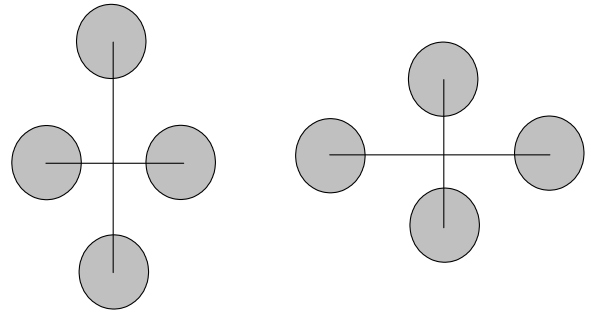


FIG. 1: The above illustrates the rearrangement dynamics during a T1 event. The centers of complimentary bubble pairs that undergo neighbor switching are joined by line segments. The two vertically connected bubbles become neighbours(N) from being next-nearest neighbours(NN), symbolized by $NN \rightarrow N$, and vice-versa for the horizontal bubbles, denoted by $NN \leftarrow N$.

In addition to shear induced T1 events, flowing foams are subject to a number of other phenomenon such as drainage, aging, coarsening and T2 events (the disappearance of a bubble within a foam) [8]. While these mechanisms do have an influence on the flow behaviour, their role is minimal at the short time-scales of response we are interested in. Various other studies look at the interaction of these mechanisms with flow, for example drainage-induced convection [21].

The role of T1 events resulting in flow in aqueous foams has a number of interesting implications. The spatial distribution of these events would provide clues to the distribution of internal stresses, as T1 events would be expected to occur more frequently in regions where the stresses exceed the local yield stress of the material. A similar argument may be used in regard to the orientation of the T1 events. The slippage between neighbouring

bubbles along a preferred direction indicates an orientational inhomogeneity within the material or the imposed forces. The temporal distribution of T1 rates would also be insightful into relaxation processes that occur: A burst of T1 events between periods of relative calm could indicate avalanche-type behaviour wherein stresses are built up slowly over time and released rapidly [9, 22]. And finally, a relationship between the configuration of bubbles and the spatial and temporal distribution of T1 events help build connections between the structural and dynamical properties of such materials.

In investigating these areas, it is important to develop a large statistics detailing the spatial and temporal distribution of T1 events. Though DWS [13, 14, 15, 16, 17] has been very successful in providing statistical information on individual bubble motions, there are no well-established techniques to gather data within the bulk of a three-dimensional foam at the time-scales and spatial resolution we require to track T1 events during shear. We therefore focus our attention on a two-dimensional foam, also known as a bubble raft. The bubble raft has been found to be a useful guide in the study of foams [19, 23] as well as solid materials [1, 24, 25]. Also, the impact of boundary conditions on T1 events in bubble rafts has been characterized [20]. In addition, it is helpful to initially study monodisperse bubble rafts. This makes it easier to interpret the results and eliminates complexities associated with polydispersity [24]. Such effects may include faster coarsening rates, the development of spatial inhomogeneities due to size dependent flow behaviour of individual bubbles etc. We also focus our observations in a regime when the foam is subjected to high rates of shear. It is expected that the system is not in a quasistatic regime, and the response is far from equilibrium. In contrast, prior studies have detailed the response at lower rates of strain [8, 19, 22], and the creep response of foam in which the impact of coarsening induced T1 events is studied [12].

In the next section we detail techniques of our experiments as well as image analysis. Following this, we present and discuss our results on the distribution of T1 events under steady shear.

II. EXPERIMENT AND IMAGE ANALYSIS

Our experiments utilize a layer of monodisperse bubbles floating on the surface of water undergoing shear between two counter-rotating bands. The bubbles were made in a trough containing an aqueous solution consisting of water, glycerol and miracle bubble solution in the ratio of 80%, 15% and 5% by volume respectively. A small amount of fluorescent dye, Fluorescein, was added as well to enhance imaging within our system. A steady stream of nitrogen injected into this solution using a needle was sufficient to generate a monodisperse layer of bubbles, resulting in a bubble raft.

In addition, two bands with evenly spaced gaps along

their length were positioned at the surface of the bubble monolayer with gears attached to submerged shafts. The shafts are supported by teflon bearings attached to the bottom of the trough. The bands were attached to a stepper motor through which their rate of motion could be accurately controlled. The bubbles floating in between these bands undergo linear shear. The amount of shear is quantified by $\gamma = 2L(t)/D$, where $D(=6\text{cm})$ is the width between the bands and L the distance traversed by the band in time t . Typically, the width of the band corresponds to about 20 bubble diameters. The entire trough was enclosed, and illuminated using UV lamps. The motion of the bubble raft was recorded as consecutively saved images using a CCD array. The frame rate of image capture was maintained high enough so as to identify individual bubbles between successive images.

The images captured were filtered to remove noise inherent in the CCD imaging technique as well as some optical inhomogeneities associated with the optics. The filtered images were thresholded to yield a binary image delineating the location of individual bubbles. The center positions of individual bubbles were computed as the center of mass of each of the delineated regions. A voronoi-construction was then used to construct the edges between the bubbles constituting the bubble raft. Nearest-neighbours were designated as those that shared a common edge. Next-nearest neighbors were also extracted using this information. Individual bubbles were identified based on the least displacement of bubbles between consecutive images.

The identification of Nearest-neighbors and next-nearest-neighbors between successive frames was used to establish the occurrence of T1 events: i.e. when a set of nearest neighbors became next nearest neighbors. The location of the T1 event was designated as the center of mass of the bubbles participating in the event. A more detailed account of the experimental and image analysis techniques may be found in reference [26]. The experiments are performed over a number of rates of shear, $\dot{\gamma} = d\gamma/dt$, producing a sequence of images taken at equally spaced time intervals.

III. RESULTS AND DISCUSSION

A. Spatial distribution: Slip zones, homogeneity

The T1 events are seen to be distributed uniformly between the bands in the region of interest. There is a slight increase in the number of T1 events in the vicinity of the bands. This may be attributed to pinning effects at the bands resulting in locally higher shear stresses. The spatially uniform distribution of T1 events seen in the lower plot in Fig. 2 suggests that the material properties as well as forces imposed are homogeneous when averaged over the entire period of shear.

Often, multiple T1 events occurs along a local crystalline axis of the foam as in the upper plot in Fig. 2.

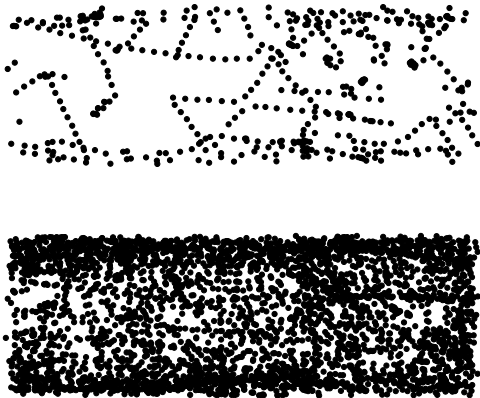


FIG. 2: The above two plots indicate the positions of T1 events over different strains. The lower figure is strained about ten times longer than the upper figure. The top figure indicates the succession of T1 events that lead to slip. The homogeneous spread of T1 events is seen in the lower figure. The increase in T1 events close to the driving bands (towards the top and bottom) are attributed to the pinning of bubbles at these boundaries.

The spatial extent of such regions may extend across the entire width of the sheared foam, indicating the role of T1 events in causing macroscopic slip and flow. Such coherent rearrangements over small γ implies that the local crystalline structure may influence the focussing of stresses as well as provide principal directions for fracture over regions of the order of the system size.

B. Orientational distribution: Anisotropy, irreversibility

In order to study the orientation of T1 events, we look at a single pair of bubbles that participate in the T1 event. This pair represents the bubbles that become nearest neighbours(N) from being next-nearest-neighbours(NN). The geometry used to define the angles of the T1 events is illustrated in Fig. 3. We focus on the angle between the x-axis (orientation of the driving bands) and the line joining nearest-neighbors as one parametrization of the orientation of the T1 events. This is plotted in Fig. 4a. We find that the orientation of T1 events shows an distribution peaked about a particular angle, which may indicate a principal shear axis. At lower rates of shear, a secondary peak is also seen. This suggests the existence of a secondary axis for shear during T1 events.

A similar measurement on the complimentary pairs of bubbles is shown in Fig. 4b. The angles corresponding to the maxima in the curves indicate the most preferred

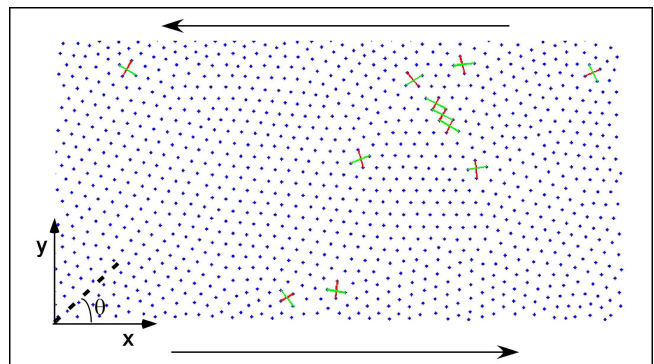


FIG. 3: The blue dots in the above plot indicate the instantaneous locations of the centers of bubbles forming the bubble raft. The red lines connect bubbles that have undergone compression, becoming nearest neighbors from being next nearest neighbors (NN \rightarrow N). The green lines connect bubbles that have undergone dilation, becoming next-nearest neighbors from being nearest neighbors initially (NN \leftarrow N). The orientation of these two events is measured by the angle (θ) the red and blue lines make with the x-axis. The horizontal arrows at the top and bottom of figure show the direction of shear imposed by the bands.

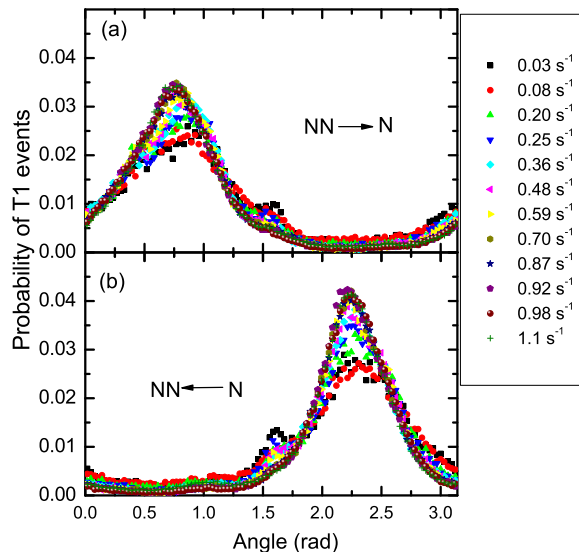


FIG. 4: The upper figure plots the angle with respect to the driving bands at which next-nearest bubbles become nearest bubbles(NN \rightarrow N). The lower figure indicates the complimentary mechanism of NN \leftarrow N. The different colours indicate plots obtained at different rates of shear.

direction of yielding through T1 events through compression and dilation. Distinct orientations for bubbles coming closer (NN \rightarrow N) and bubbles moving apart (NN \leftarrow N)

suggest an anisotropy in the internal stresses on the bubbles. The difference between the maxima of angles seen in the upper and lower plots of Fig. 4 correspond to the angle between the lines indicated in Fig. 1, further illustrating the role of local structure in directing internal stresses.

In addition to the difference in most probable angular orientation, there is also a noticeable difference in the widths of the distributions of Fig. 4. The upper plot ($NN \rightarrow N$) is observed to be broader and lower than the lower ($NN \leftarrow N$). This has important ramifications on the reversibility of T1 events. In the ideal case of reversibility, all bubbles undergoing $NN \rightarrow N$ would undergo $NN \leftarrow N$ on reversing the shear direction/time. In such a scenario, the width of angular distributions would remain unchanged between $NN \rightarrow N$ and $NN \leftarrow N$ as the two processes are symmetric under time reversal. Our observation require that such a reversal would need to occur at different ranges of angular distributions. This makes the reversibility of T1 events nontrivial in a statistical sense while placing no constraints on the reversibility of individual T1 events.

C. Temporal distribution: Rate invariance, extensivity

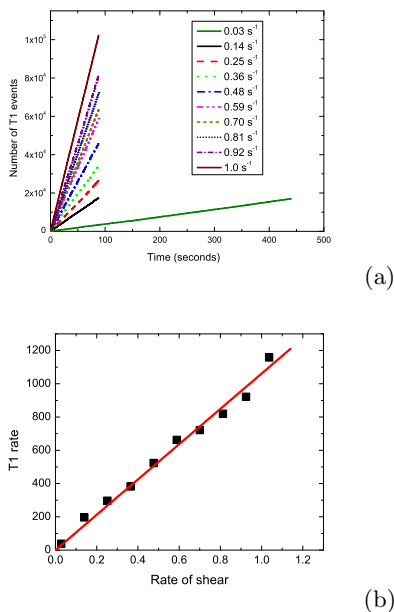


FIG. 5: (a) Number of T1 events vs. time. At the lowest rate of shear, we also include the data for longer times, illustrating the rate invariance over longer times. (b) Rate of T1 events vs. rate of shear. The solid line is a linear fit passing through the origin.

We also look at the rate at which T1 events occur. We find that even over large strains, the rate of T1 events is uniform, i.e. the rate of T1 events does not vary much during the run. It is particularly noteworthy that the rate of T1 events shows only a small deviation during shear as indicated in Fig. 5. The consistent and well defined slope in upper figure has a number of implications.

Firstly, it indicates that the rate of T1 events may be considered equivalent to a short time constraint on the dynamical evolution of the system. This implies that the response to strain at the boundaries imposes an internal consistent rate of slippage between bubbles. The rate of T1 events is seen to increase linearly with the imposed rate of shear at the boundaries.

Second, when coupled with the homogeneous spatial distribution of T1 events, it is relevant to talk about the rate of T1 events per bubble. This implies that the rate of T1 events is an extensive quantity.

IV. CONCLUSIONS AND OUTLOOK

We have undertaken a systematic study of T1 events in two-dimensional sheared aqueous foams. T1 events constitute the fundamental dynamics associated with foam flows. The study has emphasized the role of local orientation of bubbles and the resulting anisotropy in orientational distribution of T1 events. Future work will focus on connecting the observed dynamics of the T1 events with the concept of “weak zones” developed in the context of emulsions [6, 7] and the analysis of STZs in the context of model foams [3]. Also, we have demonstrated a clear correlation between the rate of T1 events and the rate of strain.

We also open many interesting avenues of investigation. For example, contrasting the statistics obtained with polydisperse bubble distributions would be useful in understanding amorphous materials. Also, the significance of structure at the ends of T1 slip zones in Fig. 2 could unravel mechanisms for fracture nucleation and termination. It would be particularly interesting to understand the origins of uneven distribution widths of angular distribution between $NN \rightarrow N$ and $NN \leftarrow N$. Designing a shear geometry that maintains symmetry in the two distributions would illustrate the influence of boundaries in determining reversibility. Finally, developing a better understanding of the connection with the results for coarsening generated T1 events in a three-dimensional foam [12] will be an important step.

Acknowledgments

This work was supported by a Department of Energy grant DE-FG02-03ED46071.

-
- [1] A. Gouldstone, K. J. V. Vliet, and S. Suresh, *Nature* **411**, 656 (2001).
- [2] M. L. Falk and J. S. Langer, *Phys. Rev. E* **57**, 7192 (1998).
- [3] C. Maloney and A. Lemaitre, *Phys. Rev. Lett.* **93**, 016001 (2004).
- [4] P. Sollich, F. Lequeux, P. Hébraud, and M. E. Cates, *Phys. Rev. Lett.* **78**, 2020 (1997).
- [5] P. Sollich, *Phys. Rev. E* **58**, 738 (1998).
- [6] A. J. Liu, S. Ramaswamy, T. G. Mason, H. Gaug, and D. A. Weitz, *Phys. Rev. Lett.* **76**, 3017 (1996).
- [7] S. A. Langer and A. J. Liu, *J. Phys. Chem B* **101**, 8667 (1997).
- [8] D. Weaire and S. Hutzler, *The Physics of Foams* (Clarendon Press, Oxford, 1999).
- [9] D. Weaire, F. Bolton, T. Herdtle, and H. Aref, *Phil. Mag. Lett.* **66**, 293 (1992).
- [10] T. Okuzono and K. Kawasaki, *Phys. Rev. E* **51**, 1246 (1995).
- [11] D. J. Durian, *Phys. Rev. Lett.* **75**, 4780 (1995).
- [12] S. Vincent-Bonnieu, R. Höhler, and S. Cohen-Addad, *Europhys. Lett.* **74**, 533 (2006).
- [13] A. D. Gopal and D. J. Durian, *Phys. Rev. Lett.* **75**, 2610 (1995).
- [14] R. Höhler, S. Cohen-Addad, and H. Hoballah, *Phys. Rev. Lett.* **79**, 1154 (1997).
- [15] S. Cohen-Addad, R. Höhler, and Y. Khidas, *Phys. Rev. Lett.* **93**, 028302 (2004).
- [16] D. J. Durian, D. A. Weitz, and D. J. Pine, *Science* **252**, 686 (1991).
- [17] J. C. Earnshaw and A. H. Jaafar, *Phys. Rev. E* **49**, 5408 (1994).
- [18] M. Dennin and C. M. Knobler, *Phys. Rev. Lett.* **78**, 2485 (1997).
- [19] M. Dennin, *Phys. Rev. E* **70**, 041406 (2004).
- [20] M. F. Vaz and S. J. Cox, *Phil. Mag. Lett.* **85**, 415 (2005).
- [21] S. J. Cox, M. D. Alonso, D. Weaire, and S. Hutzler, *Eur. Phys. J. E Soft Matter* **19**, 17 (2006).
- [22] A. A. Kader and J. C. Earnshaw, *Phys. Rev. Lett.* **82**, 2610 (1999).
- [23] T. Tam, D. Ohata, and M. Wu, *Phys. Rev. E* **61**, R9 (2000).
- [24] A. W. Simpson and P. H. Hodkinson, *Nature* **237**, 320 (1972).
- [25] L. Bragg and W. M. Lomer, *Proc. R. Soc. London, Ser. A* **196**, 171 (1949).
- [26] Y. Wang, K. Krishan, and M. Dennin, *Phys. Rev. E* **73**, 031401 (2006).